Contents lists available at ScienceDirect

Biochemistry and Biophysics Reports

Enhancing hypothiocyanite production by lactoperoxidase – mechanism and chemical properties of promotors

Jana Gau [a], Paul-Georg Furtmüller [b], Christian Obinger [b], Jürgen Arnhold [a,c], Jörg Flemmig [a,c,*]

[a] Institute for Medical Physics and Biophysics, Medical Faculty, University of Leipzig, Härtelstraße 16-18, 04107 Leipzig, Germany
[b] Department of Chemistry, Division of Biochemistry, University of Natural Resources and Life Sciences (BOKU) Vienna, Muthgasse 18, 1190 Vienna, Austria
[c] Translational Centre for Regenerative Medicine (TRM) Leipzig, University of Leipzig, Philipp-Rosenthal-Straße 55, 04103 Leipzig, Germany

ARTICLE INFO

ABSTRACT

Background: The heme enzyme lactoperoxidase is found in body secretions where it significantly contributes to the humoral immune response against pathogens. After activation the peroxidase oxidizes thiocyanate to hypothiocyanite which is known for its microbicidal properties. Yet several pathologies are accompanied by a disturbed hypothiocyanite production which results in a reduced immune defense.
Methods: The results were obtained by measuring enzyme-kinetic parameters using UV–vis spectroscopy and a standardized enzyme-kinetic test system as well as by the determination of second order rate constants using stopped-flow spectroscopy.
Results: In this study we systematically tested thirty aromatic substrates for their efficiency to promote the lactoperoxidase-mediated hypothiocyanite production by restoring the native ferric enzyme state. Thereby hydrophobic compounds with a 3,4-dihydroxyphenyl partial structure such as hydroxytyrosol and selected flavonoids emerged as highly efficient promotors of the (pseudo-)halogenating lactoperoxidase activity.
Conclusions: This study discusses important structure-function relationships of efficient aromatic LPO substrates and may contribute to the development of new agents to promote lactoperoxidase activity in secretory fluids of patients.
Significance: This study may contribute to a better understanding of the (patho-)physiological importance of the (pseudo-)halogenating lactoperoxidase activity. The presented results may in future lead to the development of new therapeutic strategies which, by reactivating lactoperoxidase-derived hypothiocyanite production, promote the immunological activity of this enzyme.

1. Introduction

Lactoperoxidase (LPO) belongs to the immunological relevant chordata peroxidases [1]. While the related enzymes myeloperoxidase (MPO) and eosinophil peroxidase (EPO) are expressed in immune cells, LPO is secreted by mucosal glands to body fluids like milk, saliva, tears and airway secretions [2–4]. The immunological function of all three enzymes is mainly attributed to their (pseudo-)halogenating activity [3,5,6]. While all three peroxidases easily oxidize iodide and thiocyanate, bromide is only oxidized by EPO and MPO and at neutral pH and the oxidation of chloride is only known for MPO [7–9]. Considering low iodide (2 µM or less) and much higher thiocyanate concentrations (up to 6 mM in saliva) [10], in secretions the two-electron oxidation of SCN^- by LPO clearly dominates. Thereby hypothiocyanite (^-OSCN) is formed, which is well known for its microbicidal properties [10]. In fact, due to its lower reactivity as compared to e.g. hypochlorous acid (HOCl), hypothiocyanite is more efficient in entering bacterial biofilms [6]. Yet the ^-OSCN-production by LPO is known to be impaired under pathological conditions like cystic fibrosis or at neonatal pathologies, which results in a disturbed immune defense against pathogens [3,11].

Chordata peroxidases are known to catalyze two- and one-

electron oxidation reactions [2]. Both reaction cycles are initiated by hydrogen peroxide-mediated oxidation of the ferric enzyme to Compound I (i.e. oxoiron(IV)porphyryl radical, $^{+\bullet}$Por-Fe^{IV}=O). In the halogenation cycle Compound I is directly reduced by halides or thiocyanate to the Fe(III) resting state, whereas in the peroxidase cycle Compound I is reduced in two one-electron reduction steps. Here, Compound II (i.e. oxoiron(IV), Por-Fe^{IV}-OH) is formed as an intermediate state which does not participate in the (pseudo-)halogenating activity [2,5,12]. Since the rate-limiting step within the peroxidase cycle is Compound II reduction to the ferric state, typically Compound II accumulates during reaction [3,5,13]. In addition to peroxidase substrate-mediated Compound I reduction to Compound II, in the absence of exogenous electron donors or at very low concentration of the substrates, the protein moiety of LPO can donate electrons thereby forming an alternative Compound I* (with remote radical site and Compound II-like UV–vis spectral signature) [10]. As a consequence, at pathological low SCN$^-$ concentrations (e.g. at cystic fibrosis) Compound II and Compound I* will accumulate, with the latter leading to oxidative damage of LPO and, finally, to enzyme inactivation [11,14]. Formation of Compound I* and accumulation of Compound II of LPO (or MPO) can be overcome in the presence of good one-electron donors that efficiently react with both Compound I and Compound II [15,16]. This restores the ferric enzyme form and, thus, promotes the (pseudo-)halogenating enzyme activity. For LPO, we could recently show that substrates from olive tree (*Olea europaea* L.) leaves having a 3,4-dihydroxyphenyl partial structure are good re-activators of the $^-$OSCN production by LPO [12]. The same holds for a subsequent study on motherwort (*Leonurus cardiaca* L) [17]. Both plants were used in traditional medicine as a remedy against e.g. inflammatory diseases [18,19]. However, so far a systematic and detailed mechanistic investigation of kinetic parameters including the direct interaction of these molecules with all relevant catalytic redox intermediates of LPO was not performed.

This study describes the mechanism of re-activation of the (pseudo-)halogenating activity of LPO by benzoic acid derivatives carrying hydroxyl and methoxy groups at different positions of the aromatic ring as well as by selected phenylethanoids, cinnamic acid derivatives and flavonoids. Steady-state kinetic parameters for the peroxidase activity are presented and discussed with respect to chemical properties (e.g. hydrophobicity) of these molecules. Finally, second order rate constants for the interaction of selected aromatic substrates with LPO Compound I and II were determined by multi-mixing stopped-flow spectroscopy. Both, high degree of hydrophobicity and the presence of a 3,4-dihydroxyphenyl partial structure are important for efficient reduction of LPO Compound II and thus for promotion of its (pseudo-)halogenating activity of LPO.

2. Materials and methods

2.1. Materials

Lactoperoxidase from bovine milk was obtained as a lyophilized powder ($\geq$ 200 U/mg) from Sigma-Aldrich, Steinheim, Germany. Aliquots of the enzyme (5 μM) were prepared in phosphate buffered saline pH 7.4 (PBS, Sigma-Aldrich) and stored at -25 °C. If not otherwise stated final enzyme concentrations of 5 nM (0.08 U/mg) were used.

Lactoperoxidase-mediated $^-$OSCN-formation was quantified by following the oxidation of 5-thio-2-nitrobenzoic acid (TNB) at 412 nm using a Varian Cary 50 UV/vis–spectrophotometer (Mulgrave, Australia). The final TNB concentration in the reaction mixture was 50 μM. Thiocyanate and hydrogen peroxide were used at final concentrations of 2 mM and 20 μM or 80 μM,

respectively. Hydrogen peroxide working solution was freshly prepared each day from a 30% stock solution by dilution in Millipore water and stored at 4 °C until use. The concentration of H$_2$O$_2$ was determined at 230 and 240 nm ($\varepsilon_{230}=74$ M^{-1} cm^{-1} ε_{240} $=43.6$ M^{-1} cm^{-1}) [20]. Dibasic sodium phosphate, sodium citrate and sodium chloride (citrate phosphate buffer preparation), 5,5′-dithiobis-(2-nitrobenzoic acid) (DTNB, $\geq$ 98%) for TNB preparation, KSCN ($\geq$ 99%), H$_2$O$_2$ and tryptophan ($\geq$ 99%) were obtained from Sigma-Aldrich.

Benzoic acid ($\geq$ 99.5%), 2-hydroxybenzoic acid ($\geq$ 99%), 3-hydroxybenzoic acid ($\geq$ 99%), 4-hydroxybenzoic acid ($\geq$ 99%), 2,3-dihydroxybenzoic acid ($\geq$ 99%), 2,4-dihydroxybenzoic acid ($\geq$ 97%), 2,5-dihydroxybenzoic acid ($\geq$ 99.5%), 2,6-dihydroxybenzoic acid ($\geq$ 97.5%), 3,4-dihydroxybenzoic acid ($\geq$ 97%), 3,5-dihydroxybenzoic acid ($\geq$ 97%), 3-hydroxy-4-methoxybenzoic acid ($\geq$ 97%), 4-hydroxy-3-methoxybenzoic acid ($\geq$ 97%), 3,4-dimethoxybenzoic acid ($\geq$ 99%), 2,3,4-trihydroxybenzoic acid ($\geq$ 97%), 2,4,6-trihydroxybenzoic acid monohydrate ($\geq$ 90%) 2,4,5-trihydroxybenzoic acid, 3,4,5-trihydroxybenzoic acid ($\geq$ 98.5%), cinnamic acid ($\geq$ 99%), *o*-coumaric acid ($\geq$ 97%), *m*-coumaric acid, ($\geq$ 99%), *p*-coumaric acid ($\geq$ 98%), caffeic acid ($\geq$ 8%), ferulic acid ($\geq$ 99%), isoferulic acid ($\geq$ 97%), sinapic acid ($\geq$ 98%), 3,4-dimethoxycinnamic acid ($\geq$ 99%) *m*-tyrosol ($\geq$ 99%), apigenin ($\geq$ 98%), eriodictyol ($\geq$ 95%), naringenin ($\geq$ 98%), luteolin ($\geq$ 98%), ($-$)-epicatechin ($\geq$ 90%), taxifolin ($\geq$ 85%), chrysin ($\geq$ 98%) and quercetin ($\geq$ 95%) were purchased from Sigma-Aldrich. Hydroxytyrosol ($\geq$ 98%) was obtained by Tokyo Chemical Industries Co., Ltd., Tokyo, Japan, and tyrosol ($\geq$ 98%) from Biopurify Phytochemicals Ltd.

Apigenin, naringenin were dissolved in DMSO (Sigma-Aldrich). The final DMSO concentration in the test system did not exceed 1% (v/v). Control measurements showed no effect of such a solvent concentration on the enzyme activity. All other test substances were dissolved in cold or hot PBS (pH 7.4), depending on their solubility. Stock solutions of 1–20 mM were prepared. Final concentrations up to 5 mM were tested.

2.2. Hypothiocyanite-dependent TNB degradation

All enzyme-kinetic measurements were performed in PBS pH 7.4 at 37 °C using a microplate reader Tecan Infinite 200 PRO (Männedorf, Switzerland). Control measurements in the absence of SCN$^-$ or in the sole presence of H$_2$O$_2$ were performed to determine the contribution of the direct LPO-mediated TNB degradation and the H$_2$O$_2$-mediated oxidation of TNB, respectively. From these data the initial LPO-mediated $^-$OSCN formation rate was calculated by considering the molar absorption coefficient of TNB ($\varepsilon_{412}=14.100$ M^{-1} cm^{-1}) [21], the length of the optical pathway (0.73 cm) and the stoichiometry of the $^-$OSCN-mediated TNB oxidation [12]. For all tested substances a clear dependence between substrate concentrations and $^-$OSCN formation rate was found, often showing a Michaelis-Menten-like correlation. Thus, Lineweaver-Burk plots were used to determine enzyme kinetic parameters (V_{max}, K_m, k_{cat}, specificity constant).

All measurements were performed at least in triplicate. Before calculating the LPO-mediated $^-$OSCN formation rate the initial TNB degradation in the absence of thiocyanate (only LPO and H$_2$O$_2$) was subtracted from the TNB degradation rate determined for the whole LPO–H$_2$O$_2$–SCN$^-$ system. This was necessary to consider the degradation of TNB by the LPO–H$_2$O$_2$ system in the absence of SCN$^-$ [12]. Thereby while the mean values were subtracted the corresponding standard deviations were calculated according to the law of error propagation. Significance was tested using two tailed *t*-test. The indicated stars correspond to *p* values below 0.05 (*), 0.01 (**) and 0.001 (***), respectively. As the K_m and V_{max} values of the tested substances were determined via a

Lineweaver-Burk plot the given standard deviations correspond to the R^2 value obtained during the linear fit of the experimental data.

2.3. Stopped-flow kinetic measurements

For selected aromatic compounds second order rate constants for their reaction with LPO Compound I and II were determined by performing stopped-flow kinetic measurements. Thereby an SX-18 MV apparatus from Applied Photophysics (Leatherhead, United Kingdom) was used. Briefly, LPO was premixed with a two-fold excess of H_2O_2 in the aging loop for 150 ms [9]. Afterwards the substrate was added and spectral changes were followed for 10–40 s. All measurements were performed in 15 mM phosphate buffer, pH 7.4 at 25 °C. An overview over the spectral changes between 200 and 740 nm was obtained by using a diode array detector. Thereby the first spectrum was obtained after 5 ms and subsequent spectra were recorded for 10 s at logarithmic time intervals. Final concentrations were 2 μM LPO, 4 μM H_2O_2 and 2–40 μM substrate.

In order to determine the second order rate constants for the one-electronic oxidation of the substrates by LPO Compound I and II measurements were performed with 1 μM LPO and 2 μM H_2O_2 (final concentrations) under pseudo-first order conditions (at least 5-fold substrate excess over LPO). Changes in the absorbance were followed at the Soret maximum of LPO Compound II (431 nm) by monitoring 2000 data points at logarithmic time intervals for 2–40 s (total measuring time). For each substrate concentration data from at least three independent measurements were averaged. Both the initial increase in absorbance at 431 nm (Compound II formation) as well as its subsequent decrease (Compound II reduction) were fitted to single or double exponential functions, respectively, to obtain k_{obs} values. After plotting k_{obs} values against the substrate concentration the apparent second-order rate constant could be calculated from the slope of the linear plot. Again the given standard deviation corresponds to the R^2 value obtained during the linear fit of the experimental data. For selected measurements LPO Compound II was pre-formed by pre-incubating LPO with H_2O_2 in the presence of tryptophan (5-fold excess over the enzyme) for 3 s before the addition of substrate [22].

3. Results

3.1. Setup of the test system

First, we investigated the formation of $^-$OSCN by the LPO–H_2O_2 system in PBS at 37 °C in the presence of 2 mM SCN$^-$. This concentration corresponds to typical values found in saliva. Two concentrations of H_2O_2 were applied: 20 μM and 80 μM. The first value is close to the estimated range for hydrogen peroxide in saliva (8–14 μM) [23]. The value of 80 μM was used to simulate pro-inflammatory conditions. Formation of $^-$OSCN was followed using the TNB assay monitoring the absorbance decrease at 412 nm. The thiolate form of TNB interacts efficiently with $^-$OSCN, the second order rate constant of this reaction is 4.37×10^5 M^{-1} s^{-1} at pH 7.4 [24]. Previous investigations revealed also a degradation of TNB by H_2O_2 alone or H_2O_2 and LPO in the absence of SCN$^-$, whereby both systems exhibited nearly the same effect [12]. Fig. 1 depicts the impact of these side reactions showing the TNB degradation rates explored for 20 μM and for 80 μM H_2O_2 for the full LPO–H_2O_2–SCN$^-$ system (black columns) as well as for the control systems LPO+H_2O_2 without SCN$^-$ (gray columns) and H_2O_2 alone (white columns). As shown in Supplementary Fig. 1 the impact of 200 μM H_2O_2 on the (pseudo-) halogenating was comparable to that of 80 μM. Only at un-
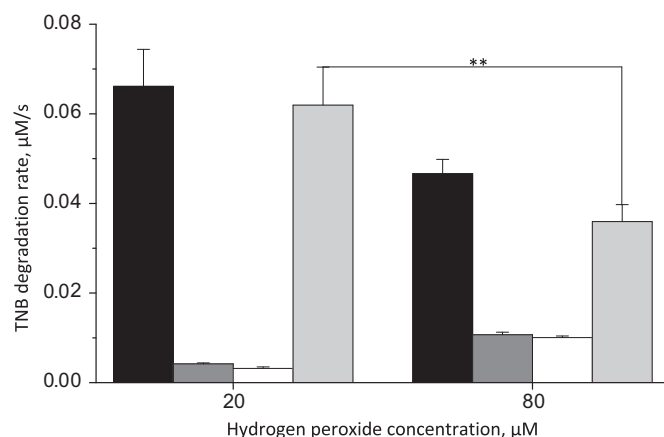

Fig. 1. Lactoperoxidase-mediated TNB degradation. The effect of low and high H_2O_2 concentrations on the (pseudo-)halogenating enzyme activity was tested at 37 °C and pH 7.4. Thereby (pseudo-) physiological conditions in the oral cavity were imitated by using 5 nM LPO and 2 mM SCN$^-$. The columns correspond to the sole presence of H_2O_2 (white), the additionally presence of LPO (gray) and the whole LPO–H_2O_2–SCN$^-$ system (black), respectively. The fourth column (light gray) shows the corresponding net effect of the $^-$OSCN mediated TNB degradation. At higher H_2O_2 concentrations a significant lower net LPO activity was found. Mean and standard deviation of $n=3$–6 experiments are given.

physiologically high concentrations a further decrease of the $^-$OSCN production by the enzyme was observed.

At each hydrogen peroxide concentration the obtained values were nearly identical for both control systems. Thus, a contribution of activated heme states of LPO to the TNB degradation can be excluded. The net $^-$OSCN-mediated TNB degradation (light gray columns) was calculated by subtracting the initial rate observed in the LPO–H_2O_2 control from the full system and always accounted for most of the effects observed in the full system (93.7% at 20 μM and 77.1% at 80 μM). Yet with increasing H_2O_2, the value for the latter declined while the values for both control systems increased. Thus, the calculated net $^-$OSCN-mediated TNB degradation rate significantly decreases (0.036 ± 0.004 μM/s at 80 μM H_2O_2 compared to 0.062 ± 0.009 μM/s at 20 μM H_2O_2), thereby reflecting accumulation of enzyme states of LPO such as Compound I* or Compound II, which are unable to oxidize SCN$^-$. These findings are in line with our previous studies on LPO, where only 100 μM SCN$^-$ were used [12].

In the next series of experiments we tried to restore the (pseudo-)halogenating activity of LPO by applying aromatic substrates. In these enzyme-kinetic studies, 5 nM LPO, 2 mM SCN$^-$, 80 μM H_2O_2 and varying concentrations of substrates were used. The single steps conducted to evaluate the effect of aromatic substrates on the $^-$OSCN-producing LPO activity are shown in Fig. 2 using the example of eriodictyol. The time traces depicted in Fig. 2A correspond to 0 μM (light gray), 0.1 μM (gray) and 5 μM (black) of the flavonoid. The addition of H_2O_2 to start the reaction is indicated by the arrow. Thereby in the full LPO–H_2O_2–SCN$^-$ system (continuous lines) a clear concentration-dependent acceleration of the TNB degradation by the flavonoid was observed while in the absence of SCN$^-$ (dashed lines) no effect was found. This proves that the increased TNB degradation really emerges from $^-$OSCN produced by LPO. Furthermore it rules out any direct contribution of eriodictyol to the TNB oxidation.

From the linear drop in absorbance the initial LPO-mediated $^-$OSCN formation rate was calculated and plotted against the eriodictyol concentration (Fig. 2B). While in the absence of this flavonoid a rate of only 0.016 ± 0.002 μM/s was observed, in the presence of 50 nM eriodictyol the initial $^-$OSCN formation was already significantly higher (0.032 ± 0.004 μM/s). With increasing flavonoid concentrations continuously raising values for the
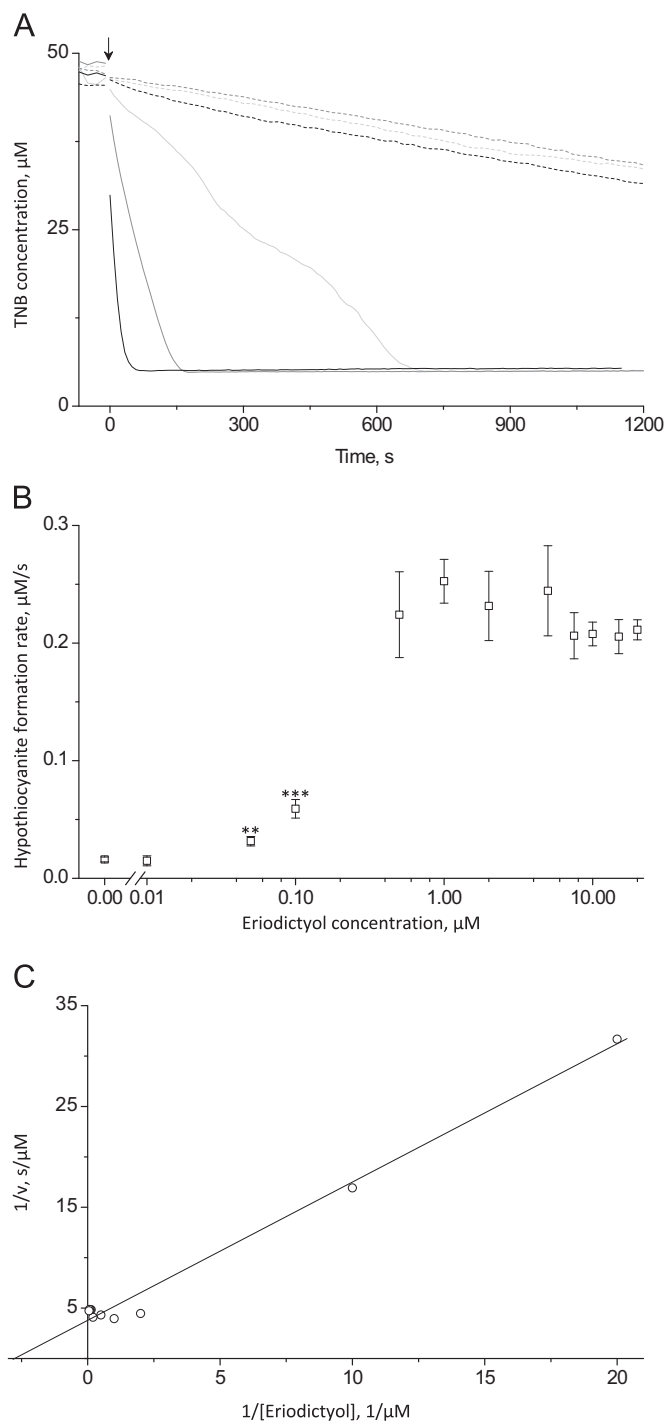
Fig. 2. Example for the modulation of the LPO-mediated TNB degradation. The effect of eriodictyol was tested at 37 °C and pH 7.4 using 5 nM LPO, and 2 mM SCN$^-$ (continuous lines). The reaction was started by adding 80 μM H$_2$O$_2$ (arrow). As shown in (A) while in the absence of the flavonoid (light gray) only a slow drop in the absorbance was observed, 0.1 μM (gray) and 5 μM (black) eriodictyol considerably accelerated the TNB degradation. This effect was not observed in the absence of SCN$^-$ (dashed lines). The plot of the initial $^-$OSCN formation rate versus the eriodictyol concentration (B) revealed an optimum flavonoid concentration of about 1 μM. At higher concentration the (pseudo-) halogenating LPO activity slightly decreased. A reciprocal re-plot of the data according to Lineweaver-Burk (C) yielded a linear dependence. From the intersection of the curve with the x- and y-axis K_m and V_{max} values of 0.358 ± 0.005 μM and 0.262 ± 0.003 μM/s, respectively, were obtained. Mean and standard deviation of n=3 experiments are given.

(pseudo-)halogenating LPO activity were found up to about 1 μM eriodictyol where a 16-fold higher rate was observed (0.253 ± 0.019 μM/s) as compared to the control. At very high

flavonoid concentrations (5–20 μM) the rate slightly (but not significantly) diminished. As shown in Fig. 2C the reciprocal re-plot of these data according to Lineweaver-Burk yielded a nearly linear dependence. The enzymatic parameters were obtained from the intercept of this curve with the x-axis ($-1/K_m$) and the y-axis ($1/V_{max}$), respectively. Thereby for K_m and V_{max} values of 0.4 ± 0.0 μM and 0.26 ± 0.00 μM/s, respectively, were determined. The standard deviation was calculated by taking into account the R^2 value of the linear curve fit. Considering the used enzyme concentration (5 nM), a k_{cat} value ($V_{max}/[E]$) of 52.4 s^{-1} and a specificity constant (k_{cat}/K_m) of 146.41 μM^{-1} s^{-1} were calculated for eriodictyol.

We also tested the concentration-dependent promotion of the (pseudo-)halogenating LPO activity by eriodictyol in the presence of only 20 μM H$_2$O$_2$ (Supplementary Fig. 2). Thereby the obtained K_m value (≈ 0.3 μM) roughly meets the data obtained in the presence of 80 μM H$_2$O$_2$, proving that the K_m value is a suitable parameter for the affinity of the substrates to the enzyme. In contrast the V_{max} value (≈ 1.3 μM/s) is only about half as high. At 0.5 μM eriodictyol the $^-$OSCN production rate (0.13 ± 0.02 μM/s) was about four to five times higher as compared to the value obtained in the absence of the flavonoid (0.03 ± 0.00 μM/s). In contrast at 80 μM H$_2$O$_2$ the same amount of eriodictyol accelerated the $^-$OSCN production from 0.02 ± 0.00 μM to 0.22 ± 0.04 μM (11 times).

3.2. Evaluation of the optimal ligand structure

Based on preliminary results for the testing of possible LPO activity-regenerating substrates in medical plants [12], we now focused on substances with a mono- or polyhydroxylated phenyl moiety and varied both the hydroxylation pattern and the residue at the C1 position. The results shown in Fig. 3 always correspond to the K_m values (black circles) and the V_{max} values (white squares) obtained from enzyme-kinetic measurements with the aromatic substrates. Efficient promoters of the (pseudo-)halogenating LPO activity are expected to exhibit a low K_m and a high V_{max} value. While in Fig. 3A, C and E the results of the enzyme-kinetic measurements are shown, in Fig. 3B, D and F the corresponding basic chemical structure of the tested substance class is displayed.

The most extensive studies were performed using benzoic acid derivatives (carboxyl group at the C1 position) by testing nearly all possible hydroxylation patterns of the phenyl ring (Fig. 3A). Regarding the monohydroxylated derivatives, 3-hydroxybenzoic acid (K_m: 144.2 ± 28.9 μM, V_{max}: 0.18 ± 0.04 μM/s) emerged as the most promising candidate. In this series the highest V_{max} was measured for 3,4-dihydroxybenzoic acid (0.30 ± 0.00 μM/s). Introduction of a third hydroxyl group did not further improve the rate of hypothiocyanite production by LPO (Table 1).

Finally, the importance of the 3,4-dihydroxylation pattern for binding of the aromatic molecule to the oxidation site in LPO was confirmed by introduction of methoxy groups at the respective positions, which resulted in significant increase of the corresponding K_m values. Interestingly, the monomethoxylated electron donors still exhibited V_{max} values similar to 3,4-dihydrohybenzoic acid (Table 1).

We also tested phenylethanoids (ethanol moiety at the C1 position) (Fig. 3C). Thereby we focused on those with a 3-hydroxylation (m-tyrosol), a 4-hydroxylation (tyrosol) or a 3,4-dihydroxylation (hydroxytyrosol) pattern. All substances showed considerably lower K_m values (1.6–4.5 μM) as compared to their benzoic acid equivalents, indicating a better binding of these substances in the substrate channel of LPO. For the 3-hydroxylation and for the 3,4-dihydroxylation the obtained V_{max} values (0.14 ± 0.00 μM/s and 0.34 ± 0.01 μM/s, respectively) were roughly comparable to the data obtained for their benzoic acid equivalents.
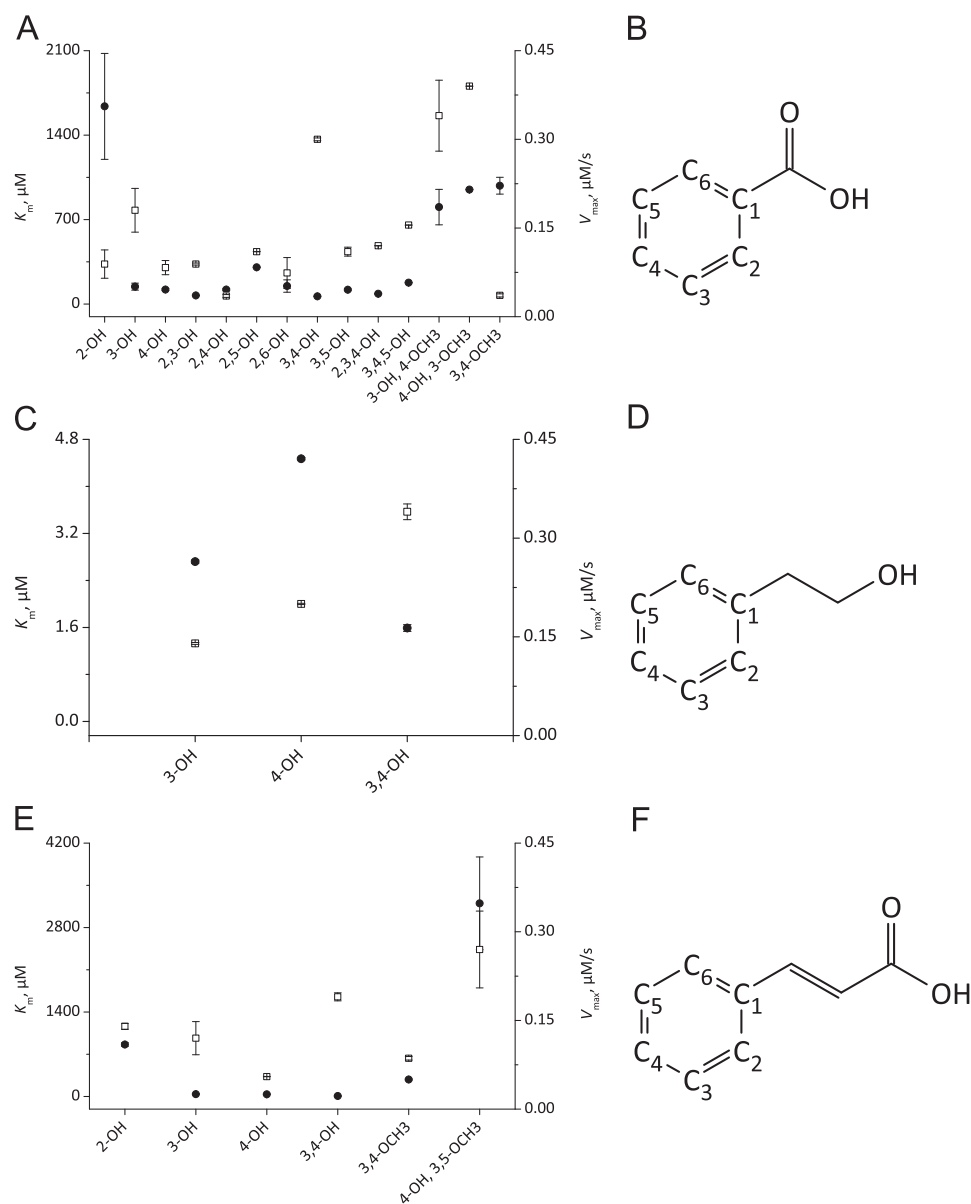
Fig. 3. K_m and V_{max} values of aromatic compounds. The shown enzymatic parameters correspond to benzoic acid derivatives (A), phenylethanoids (C) and cinnamic acid derivatives (E), respectively while in (B), (D) and (F) the corresponding basic chemical structures are shown. Regarding the enzyme-kinetic data the black circles represent the K_m values while the V_{max} values are shown as white squares. For all substance classes compounds with a 3,4-dihydroxyphenyl moiety emerged as the most efficient LPO activity regenerators. The given standard deviations correspondent to the R^2 value observed during the linear fit of the experimental data according to Lineweaver-Burk. Mean and standard deviation of $n = 3$–9 experiments are given.

This nicely illustrates that while the substitution pattern at the C1 position affects the binding of the substrates, there oxidizability by LPO only depends on the hydroxylation pattern of the phenyl moiety.

The data shown in Fig. 3E correspond to the testing of cinnamic acid derivatives (acrylic acid at the C1 position). Again the lowest K_m values were found for the 3-hydroxylated (*m*-coumaric acid), 4-hydroxylated (*p*-coumaric acid) and 3,4-dihydroxylated (caffeic acid) compounds, while for the other test substances a much weaker affinity to the enzyme was obtained. For caffeic acid the relatively low K_m value (as compared to the other cinnamic acid derivatives) coincided with a relatively high V_{max} value (0.19 ± 0.01 µM/s), again confirming the important role of the 3,4-dihydroxylation for the reactivation of LPO activity.

As the last class of chemical compounds we tested flavonoids (Fig. 4). Thereby we focused on compounds with an 3′,4′-dihydroxylation at the B ring but also included substances with a 4′-monohydroxylated B ring. While in Fig. 4A the obtained enzyme-kinetic data are summarized, Fig. 4B shows the basic chemical structure shared by all tested flavonoids and Fig. 4C points out the chemical differences between the compounds. All tested flavonoids showed quite low K_m values (0.1–1.7 µM). This implies a quite good binding of all tested flavonoids. Compounds with a 3′,4′-dihydroxylated B ring (eriodictyol, luteolin, taxifolin, (−)-epicatechin, quercetin) also showed high V_{max} values (0.21 -0.51 µM/s), indicating an excellent reactivity with the active center of LPO. In contrast, for the monohydroxylated compounds naringenin and apigenin lower V_{max} values were found (0.1 ± 0.00 µM/s and 0.07 ± 0.00 µM, respectively). Considering both the K_m and the V_{max} value the flavanon eriodictiol and the flavon luteolin emerged as the best substances for the regeneration of the (pseudo-)halogenating LPO activity throughout the whole study.

Table 1
Enzymatic and chemical properties of the aromatic compounds tested for their reactivating effect on the $^-$OSCN production by LPO.

Substance class/ compound	K_m, µM	V_{max}, µM/s	k_{cat}, 1/s	k_{cat}/K_m, 1/µM s	logD Value
Benzoic acid derivatives					
2-OH	1638.4 ± 439.3	0.09 ± 0.02	17.8	0.11	−1.09
3-OH	144.2 ± 28.9	0.18 ± 0.04	36.5	0.25	−1.47
4-OH	119.6 ± 8.1	0.08 ± 0.01	16.7	0.14	−1.33
2,3-OH	71.3 ± 1.3	0.09 ± 0.00	17.9	0.25	−1.35
2,4-OH	119.6 ± 8.3	0.04 ± 0.00	7.0	0.06	−1.56
2,5-OH	304.2 ± 0.1	0.11 ± 0.00	22.4	0.07	−1.58
2,6-OH	149.1 ± 51.4	0.07 ± 0.03	14.8	0.10	−0.91
3,4-OH	63.9 ± 51.4	0.30 ± 0.01	59.2	0.93	−1.73
3,5-OH	118.0 ± 7.9	0.11 ± 0.01	22.7	0.19	−1.92
2,3,4-OH	84.8 ± 0.0	0.12 ± 0.00	24.5	0.29	−1.69
3,4,5-OH	176.8 ± 0.0	0.16 ± 0.00	30.9	0.18	−2.08
3-OH, 4-OCH₃	803.5 ± 147.2	0.34 ± 0.06	67.7	0.08	−1.51
4-OH, 3-OCH₃	948.4 ± 0.2	0.40 ± 0.00	78.5	0.08	−1.49
3,4-OCH₃	980.8 ± 69.8	0.04 ± 0.00	7.2	0.01	−0.80
Phenylethanoids					
3-OH	2.7 ± 0.0	0.14 ± 0.00	28.4	10.56	0.62
4-OH	4.5 ± 0.0	0.20 ± 0.00	39.0	8.73	0.62
3,4-OH	1.6 ± 0.1	0.34 ± 0.01	67.0	42.10	0.02
Cinnamic acid derivatives					
2-OH	861.3 ± 30.8	0.14 ± 0.01	27.7	0.03	−1.35
3-OH	37.8 ± 8.9	0.12 ± 0.03	24.0	0.63	−1.16
4-OH	35.1 ± 0.1	0.06 ± 0.00	11.0	0.31	−1.13
3,4-OH	6.9 ± 0.3	0.19 ± 0.01	37.2	5.40	−1.67
3,4-OCH₃	281.1 ± 9.4	0.09 ± 0.00	17.2	0.06	−0.58
4-OH, 3,5-OCH₃	3201.3 ± 763.2	0.27 ± 0.07	54.8	0.02	−1.82
Flavonoids					
Naringenin	0.2 ± 0.0	0.10 ± 0.00	19.0	102.52	2.22
Eriodictyol	0.4 ± 0.0	0.26 ± 0.00	52.4	146.41	2.17
Apigenin	0.1 ± 0.0	0.07 ± 0.00	13.1	122.32	1.26
Luteolin	0.2 ± 0.0	0.46 ± 0.04	91.6	472.14	1.17
Taxifolin	0.8 ± 0.0	0.24 ± 0.01	48.2	62.99	1.31
Quercetin	1.7 ± 0.2	0.51 ± 0.06	102.0	60.67	0.71
Epicatechin	0.6 ± 0.0	0.21 ± 0.01	41.4	68.41	0.48

Fig. 4. K_m and V_{max} values of selected flavonoids. The enzymatic parameters shown in (A) again correspond to the K_m value (black circles) and the V_{max} value (white squares) of the flavonoids. In (B) the basic chemical structure of flavonoids is given and in (C) the chemical differences between the tested flavonoids are shown. Thereby the connection between C_2 and C_3 of the C ring is indicated as single bond (SB) or double bond (DB). All flavonoids showed a quite high affinity to LPO (low K_m value). Regarding the V_{max} value those compounds with a monohydroxylation at the B ring (naringenin and apigenin) exhibited a quite weak regenerating effect on the LPO activity. In contrast the flavonoids with a 3,4-dihydroxylated B ring emerged as excellent LPO substrates. Mean and standard deviation of $n = 3-5$ experiments are given.

3.3. Chemical properties of efficient ligands

Table 1 presents the catalytic specificities (k_{cat}/K_m) of all tested compounds along with their respective logD values (obtained from ACD/ChemSketch; version 12.01) that reflect the hydrophobicity of the molecules.

In Fig. 5 those values are plotted versus the catalytic specificity. Data are shown only for 3,4-dihydroxylated (black), 3-hydroxylated (gray) or 4-hydroxylated (white) compounds since those emerged as the most promising candidates for promotion of hypothiocyanite production. For all hydroxylation patterns a positive correlation between the catalytic efficiency and logD was found. The more hydrophobic (more positive logD values) a molecule is the higher is the catalytic specificity of the corresponding hydroxylated derivatives (phenylethanoids > cinnamic acid derivatives > benzoic acid derivative). Molecules with hydroxylation at position 3 showed higher k_{cat}/K_m values compared to those having the position 4 hydroxylated. Similarly, for most of the tested flavonoids the catalytic specificity increased with increasing logD values, although the exact structure of the electron donor is important too [compare luteolin ($k_{cat}/K_m = 472.14$ 1/(µM s), logD = 1.17) with eriodictyol ($k_{cat}/K_m = 146.41$ 1/(µM s), logD: 2.17)].

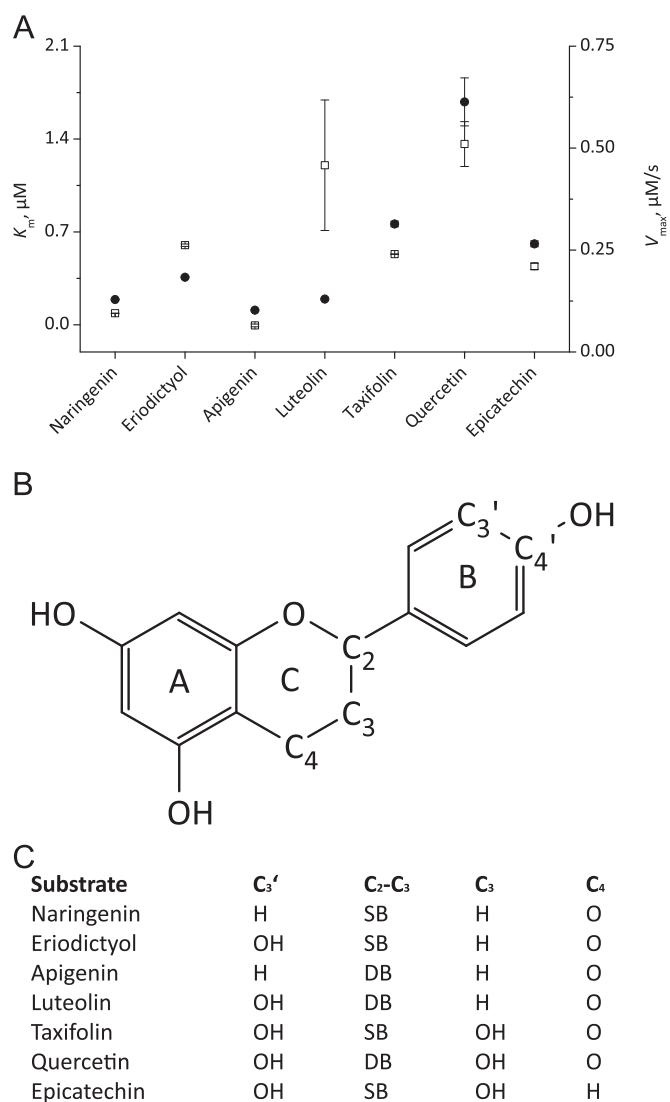On the other hand, within one substance class (underlined in gray) the highest catalytic specificity was always found for the 3,4-dihydroxylated compound, although those molecules were less hydrophobic than the monohydroxylated counterparts. This was also seen for the flavonoids apigenin and naringenin that showed lower k_{cat}/K_m values than luteolin and eriodictyol.

3.4. Determination of second order rate constants for selected ligands

The re-activation of the (pseuo)-halogenating activity of LPO by selected aromatic compounds is assumed to be caused by converting Compound II (or Compound I* that has identical UV–vis spectral signatures) to the ferric enzyme. To prove this assumption, we performed comprehensive multi-mixing stopped-flow kinetic measurements to directly study the interaction of selected substrates with the redox intermediates of LPO.

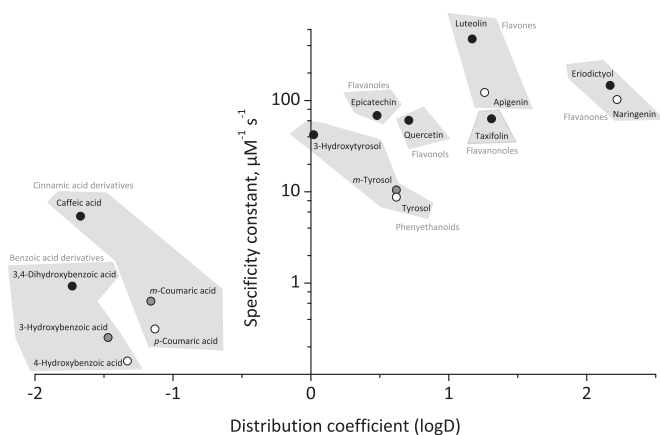Fig. 6 depicts representative spectral changes of Compound I

Fig. 5. Dependence of the enzymatic specificity constant from the distribution coefficient. Compounds with an 3,4-dihydroxy- (black), 3-hydroxy- (gray) or 4-hydroxy- (white) phenyl moiety were plotted against their logD value. Their affiliation to the different substance classes is also indicated. Among one hydroxylation pattern hydrophobic compounds (e.g. phenylethanoids) always showed stronger LPO activity-regenerating effects than hydrophilic ones (e.g. benzoic acid derivatives). Within one substance class the compounds with 3-4-dihydroxyphenyl moiety always had the strongest impact on the LPO-mediated $^-$OSCN production.

reduction to Compound II as well as Compound II reduction to ferric LPO (Fig. 6B) mediated by 3,4-dihydroxybenzoic acid. In the absence of a substrate (Fig. 6A) the Soret maximum slowly shifted from 412 to 431 nm. This transition was accompanied by characteristic spectral changes in the red spectral region (new maxima at 536 and 568 nm) and reflects the spontaneous decay of Compound I to Compound I* with Compound II-like spectral signatures [9,10,25]. In the presence of 20 μM 3,4-dihydroxybenzoic acid Compound I (bold black line) was rapidly converted to Compound II (bold gray line) within the first second with isosbestic points at 406, 465, 515 and 586 nm (Fig. 6B). Additionally, within the next 9 s (light gray bold line) a second transition took place, representing Compound II reduction to the native enzyme. The latter reaction is clearly visible from the increase of the absorbance at 412 nm as well as from characteristic isosbestic points at 423, 469 and 517 nm [9,22,25]. In the absence of the substrate (Fig. 6A) no regeneration of native LPO was observed within 10 s. Thus, 3,4-dihydroxybenzoic acid promotes both the transition of LPO Compound I to Compound II as well as the subsequent regeneration of native enzyme.

In order to determine the reaction rates for both transitions the time-dependent increase (Compound II formation, Fig. 6C) and decrease (Compound II resolution, Fig.6E) in the absorbance at 431 nm was followed. By applying double exponential (Fig. 6C) and single exponential (Fig. 6E) fitting functions to these time traces k_{obs} values were determined and re-plotted *versus* the used substrate concentrations (Fig. 6D and F). From the slope of the obtained linear correlation curve second order rate constants of $(8.09 \pm 0.12) \times 10^5 \, \mathrm{M^{-1} \, s^{-1}}$ and $(2.90 \pm 0.01) \times 10^4 \, \mathrm{M^{-1} \, s^{-1}}$ were determined for the reaction of 3,4-dihydroxybenzoic acid with LPO Compound I and II, respectively. Thereby the given errors correspond to the R^2 value obtained during the linear fit. A double-exponential equation [obtaining pseudo-first-order rate constants $k_{obs(1)}$ and $k_{obs(2)}$] was applied for fitting the transition from Compound I to Compound II (Fig. 6C). Yet the obtained values revealed that $k_{obs(1)}$ is responsible for more than 85% of the increase in the absorbance at 431 nm, whereas $k_{obs(2)}$ was significantly smaller and did not depend on the substrate concentration.

Similar experiments were performed with 3- and 4-hydroxylated and 3,4-dihydroxylated derivatives of benzoic acids, phenylethanoids and cinnamic acids (Table 2). For the determination

of the reaction rate of hydroxytyrosol with LPO Compound II it was necessary to pre-form the latter by using tryptophan (donates electrons to Compound I but very slowly to Compound II) before adding the substrate [22]. For all substance classes the highest rates (both for the Compound II formation and for its subsequent reduction to native LPO) were always found for the 3,4-dihydroxylated compound while the corresponding rates of the monohydroxylated compounds were about 10- to 100-fold lower. Generally, the hierarchy of reactivity at Compounds I and II was phenylethanoid > cinnamic acid > benzoic acid derivatives (reflecting the hierarchy in hydrophobicity, compare with Table 1).

Note that the reaction of hydroxytyrosol with LPO Compound I was too fast to be determined properly ($> 7.5 \times 10^7 \, \mathrm{M^{-1} \, s^{-1}}$). Yet both for 3,4-dihydroxybenzoic acid and for caffeic acid the reaction with Compound I was always about 30 times faster as compared to the reaction with Compound II (see ratios given in Table 2). Thus, it can be guessed that the second order rate constant for the reaction of hydroxytyrosol with LPO Compound I may be in the range of $10^7 – 10^8 \, \mathrm{M^{-1} \, s^{-1}}$. Table 2 in addition presents the ratio of rates at Compounds I and II which are smallest for the dihydroxylated derivatives, since the latter show high reactivity also with Compound II. The monohydroxylated compounds always reacted considerably slower with Compound II than with Compound I. Thereby for the benzoic acid derivatives the ratio was much lower for the 3-monohydroxylated compound (97) as compared to the 4-monohydroxylated compound (448). For the corresponding cinnamic acid derivatives the ratio was always above 500. In contrast the monohydroxylated phenylethanoids always reacted only about 100 times slower with Compound II than with Compound I.

4. Discussion

4.1. Detection of the (pseudo-)halogenating LPO activity

In this study thirty compounds from four different substance classes were tested for their capacity to enhance thiocyanate oxidation mediated by bovine lactoperoxidase. Formation of hypothiocyanite was followed using the TNB assay [12]. Thereby control measurements were included to correct for the H_2O_2-dependent TNB degradation and the direct TNB oxidation by activated LPO. There was no impact of activated heme forms of LPO on the TNB degradation. Comparable investigations on LPO activity often use ABTS, which, however, does not allow discrimination between (pseudo-) halogenating and peroxidase activity [26,27]. In fact, many of these studies are performed in the absence of SCN$^-$, and address, thus, only the peroxidase cycle [26,27]. Moreover, this method is based on the detection of accumulated ABTS$^{\bullet +}$ radicals and, therefore, not applicable for kinetic measurements [28]. In summary, the application of TNB, by including proper controls, is suitable to specifically detect the $^-$OSCN production by LPO, and to study alterations in this activity.

In contrast to our previous studies [12], we now used higher SCN$^-$ concentrations (2 mM) to reflect better the physiological conditions of the oral system [10,29]. These conditions also resulted in higher $^-$OSCN formation rates as compared to the old system (100 μM SCN$^-$). All measurements were performed in the presence of 140 mM chloride. Although Cl$^-$ concentrations may be considerably lower in the oral cavity (10–60 mM) [10] control measurements in the absence of Cl$^-$ did not lead to changes in the $^-$OSCN production (not shown), as LPO is unable to oxidize chloride [2,9]. Under the chosen conditions the application of patho-physiological relevant H_2O_2 concentrations (80 μM) inhibited the rate of TNB degradation by 42% as compared to measurements with 20 μM H_2O_2. These conditions are quite sufficient to visualize the restoration of the (pseudo-)
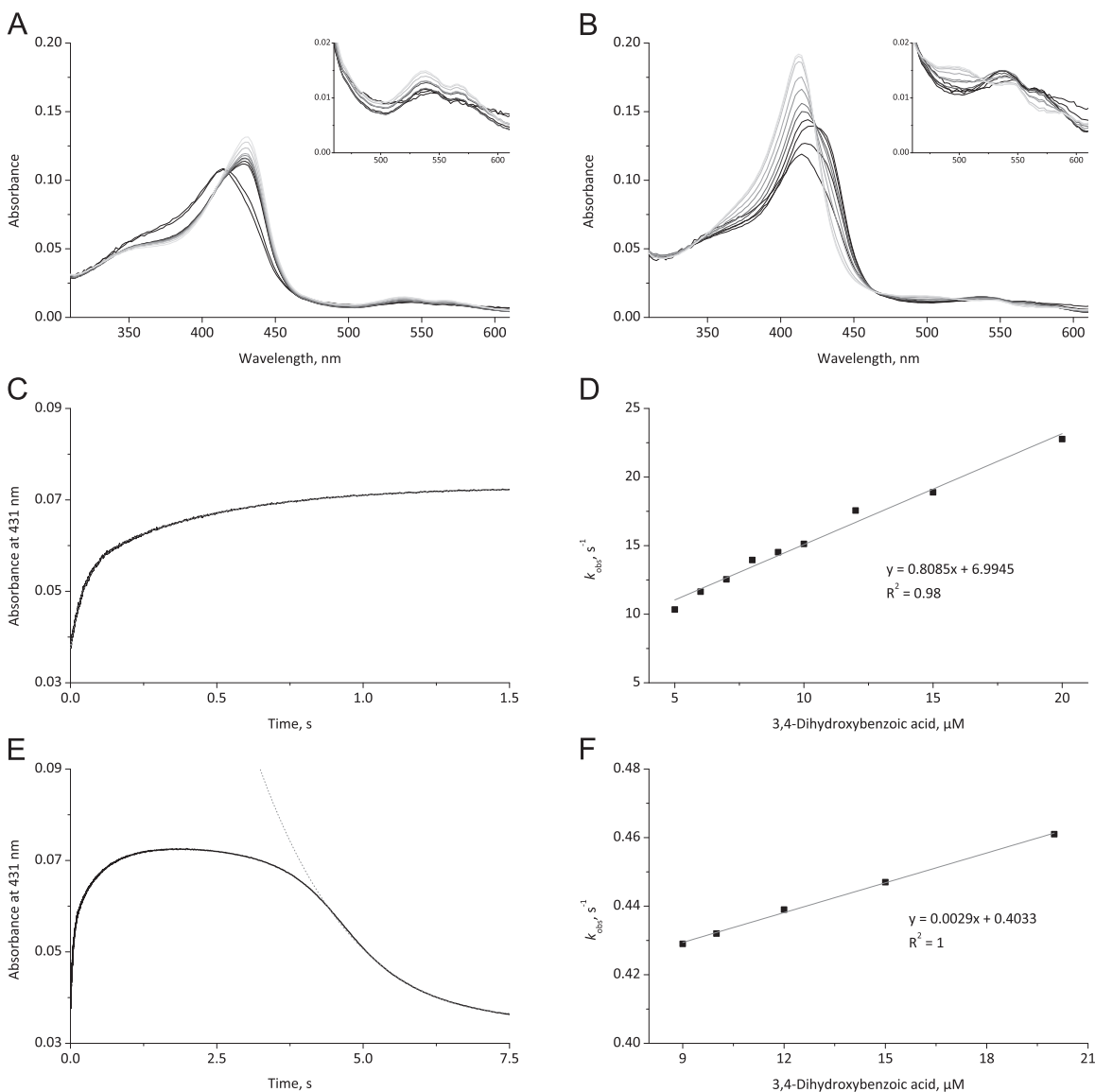
Fig. 6. Reaction rates of 3,4-dihydroxybenzoic acid with LPO. Compound I of the enzyme was pre-formed by incubating native LPO with a two-fold excess of H_2O_2 for 150 ms. Afterwards substrate was added and spectral changes were followed. While in (A) spectra were recorded after the pre-incubation of 2 μM LPO with 4 μM H_2O_2 in the absence of substrate in (B) 20 μM 3,4-dihydroxybenzoic acid were added. Spectra recorded 5 (black, bold), 66, 947 (bold), 1280, 1560, 1720, 2088, 2530, 4069, 6507 and 10,000 ms (gray, bold) after mixing are shown. In the presence of substrate (B) within the first second a quick transition from Compound I (bold black line, Soret band at 412 nm) to Compound II (bold gray line, Soret band to 431 nm, characteristic spectral changes around 550 nm) was observed which was considerably faster than in its absence (A). This reaction was followed by a slower backformation of native LPO (increase in the absorbance at 412 nm, isosbestic points at 423, 469 and 517 nm) within the next 9 s (bold light gray line) which was not observed in the negative control. For both transitions k_{obs} values were determined by following the increase (C) and decrease (E) of the absorbance at 431 nm. The data shown in (C and E) correspond to 1 μM LPO, 2 μM H_2O_2 and 20 μM 3,4-dihydroxybenzoic acid. By plotting the k_{obs} values against the substrate concentration (D and F) second order rate constants for the reaction of 3,4-dihydroxybenzoic acid with LPO Compound I (C, 8.09×10^5 M^{-1} s^{-1}) and Compound II (E, 2.90×10^4 M^{-1} s^{-1}) were determined. Mean and standard deviation of n=3 experiments are given.

halogenating activity by eriodictyol (as shown in detail) and a number of other aromatic substrates. The amount of LPO used in the study (5 nM) may be significantly lower as compared to physiological conditions (about 100 nM) but was necessary to obtain measurable $^-$OSCN formation rates [30].

4.2. Hydrogen peroxide-mediated inhibition of lactoperoxidase

There are several aspects that contribute to the reduced ability of the LPO–H_2O_2–SCN$^-$ system to generate $^-$OSCN in the absence of suitable substrates. Kinetic properties for the (pseudo-) halogenating activity of LPO are well described (see scheme 1). Hydrogen peroxide converts ferric LPO into Compound I with a rate of 1.1×10^7 M^{-1} s^{-1} at pH 7.0 and 15 °C [31]. Compound I is reduced back to the ferric LPO by SCN$^-$. The rate of this reactivation

is 2×10^8 M^{-1} s^{-1} at pH 7.0 and 15 °C [2,9]. In the absence of an exogenous electron donor Compound I undergoes a spontaneous transition into Compound I* with a rate of 2 s^{-1} at pH 7.0 and 15 °C [9,10]. Compound I* is still two oxidizing equivalents above the ferric state but contains a protein radical site instead of the porphyryl radical and thus at the heme center resembles Compound II. If not repaired (e.g. by suitable one-electron donors) this reaction leads to oxidative damage of the protein and, finally, to irreversible inhibition, as already demonstrated for several peroxidases [32]. It is yet unknown by which mechanism an excess of hydrogen peroxide affects this latter transition and contributes, thus, to an accumulation of enzyme species other than ferric LPO and Compound I.

In addition, as shown in Scheme 1 there exists a catalytic cycle between Compound II, Compound III and ferrous LPO, where H_2O_2

Table 2
Second order rate constants for the reaction of selected aromatic compounds with LPO Compound I and II at pH 7.4 and 22 °C.

Substance class/compound	Reaction rate with LPO Compound I (M^{-1} s^{-1})	Reaction rate with LPO Compound II (M^{-1} s^{-1})	Ratio
Benzoic acid derivatives			
3-OH	$(1.94 \pm 0.10) \times 10^4$	$(2.00 \pm 0.10) \times 10^2$	97
4-OH	$(8.95 \pm 0.13) \times 10^4$	$(2.00 \pm 0.12) \times 10^2$	448
3,4-OH	$(8.09 \pm 0.12) \times 10^5$	$(2.90 \pm 0.01) \times 10^4$	28
Phenylethanoids			
3-OH	$(1.06 \pm 0.18) \times 10^7$	$(1.24 \pm 0.01) \times 10^5$	85
4-OH	$(1.34 \pm 0.09) \times 10^7$	$(1.19 \pm 0.02) \times 10^5$	113
3,4-OH	–	$(3.20 \pm 0.03) \times 10^6$	–
Cinnamic acid derivatives			
3-OH	$(1.88 \pm 0.13) \times 10^6$	$(3.70 \pm 0.18) \times 10^3$	508
4-OH	$(3.52 \pm 0.07) \times 10^6$	$(5.60 \pm 0.03) \times 10^3$	629
3,4-OH	$(8.36 \pm 0.28) \times 10^6$	$(2.75 \pm 0.08) \times 10^5$	30
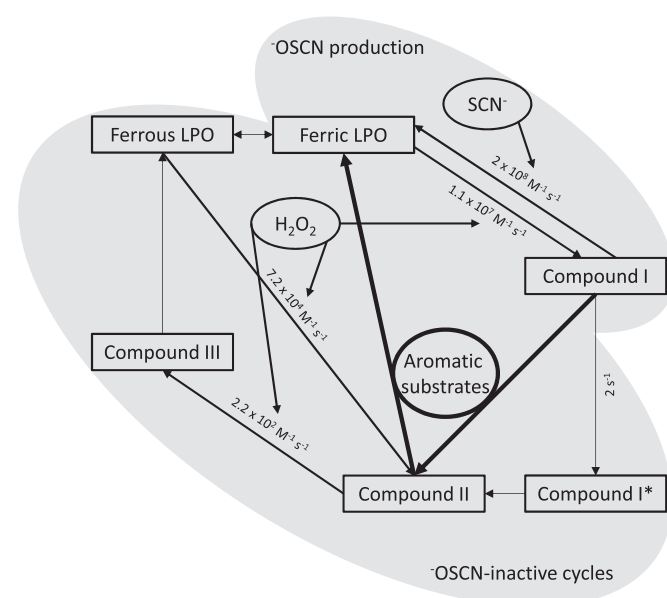
Scheme 1. Perturbation of the (pseudo-)halogenating LPO activity. After the activation of native (ferric) LPO to Compound I by H_2O_2, the enzyme quickly oxidizes SCN$^-$ to $^-$OSCN under the regeneration of native LPO. Yet especially in the presence of excess H_2O_2 this (pseudo-)halogenating activity is disturbed due to the formation of enzymatic redox intermediates which are not involved in $^-$OSCN production. This includes the spontaneous transition to Compound I* whose electronic structure at the heme center resembles Compound II. While Compound I* can lead to irreversible enzyme inhibition Compound II can further react with H_2O_2 to Compound III. The resolution of the latter by oxygen release yields the ferrous form of native LPO which is again quickly transformed to Compound II in the presence of H_2O_2. Spontaneous transitions are shown as thin arrows while standard arrows indicate reactions of LPO redox intermediates with H_2O_2 or SCN$^-$. The reaction of LPO Compound I and II with aromatic compounds is shown as bold arrows. First and second order rate constants were taken from the literature [2,9,31].

reacts with Compound II and ferrous LPO with rates of 2.2×10^2 M^{-1} s^{-1} and 7.2×10^4 M^{-1} s^{-1}, respectively, at pH 7.0 and 25 °C [2,31]. Efficient Compound II-resolving substances also avoid the formation of Compound III in the presence of excess H_2O_2 [2]. Taken together, with increasing H_2O_2 LPO is converted to enzyme forms, which are not involved in SCN$^-$ oxidation. The addition of aromatic substrates that react well with Compound II efficiently restore the (pseudo-)halogenating activity of LPO [33]. As many aromatic substrates which emerged as good re-activators of the $^-$OSCN production by LPO did not only compensate for the about 42% lower $^-$OSCN production by LPO in the presence of

80 μM H_2O_2 as compared to 20 μM H_2O_2 it can be guessed, that even at lower hydrogen peroxide concentrations a considerable amount of LPO already exists in enzymatic redox states which are not involved in $^-$OSCN production [33,34].

In fact as illustrated by Supplementary Fig. 2 even at 20 μM H_2O_2 eriodictyol considerably accelerated the (pseudo-)halogenating LPO activity: At the optimal flavonoid concentration (0.5 μM) about five times higher $^-$OSCN production rates were found, while at 80 μM H_2O_2 and the same amount of eriodictyol the effect was about twice as strong. Moreover, while at high hydrogen peroxide concentrations at even higher eriodictyol concentrations (see Fig. 2B) the $^-$OSCN production by LPO did not change significantly at low H_2O_2 (see Supplementary Fig. 2) higher amounts of the flavonoid increasingly disturbed the (pseudo-)halogenating LPO activity. Most likely the prevalence of this enzymatic cycle at 20 μM H_2O_2 is more and more disturbed by the substrate.

4.3. Properties of efficient LPO activity regenerators

In each substance class tested for promotion of hypothiocyanite production, dihydroxylation at positions 3 and 4 had the highest impact on hypothiocyanite production by LPO. This applies also to benzoic acid derivatives (k_{cat}/K_m of 3,4-dihydroxy benzoic acid is 0.93 μM^{-1} s^{-1}) although representatives from this class showed the lowest effect on thiocyanate oxidation. Among cinnamic acid derivatives and phenylethanoids, caffeic acid and hydroxytyrosol are characterized by the highest specificity constants (5.40 μM^{-1} s^{-1} and 42.10 μM^{-1} s^{-1}, respectively). Both the importance of the 3,4-dihydroxyphenyl partial structure and the role of the substrate hydrophobicity (as already observed by applying phenylethanoids) were confirmed by testing selected flavonoids. All compounds, showed a high affinity for LPO (K_m values between 0.1 and 1.7 μM) and those compounds with an 3′,4′-dihydroxylated B ring emerged as excellent reactivator of the $^-$OSCN-producing LPO activity. The highest specificity constant was found for luteolin (472.14 μM^{-1} s^{-1}).

Besides hydrophobicity the overall structure as well as physicochemical properties have to be taken into account [35]. Although the flavanon eriodictiol is even more hydrophobic than luteolin, it showed a lower specificity constant (146.41 μM^{-1} s^{-1}), maybe due to its non-planar structure. Moreover, while the presence of a hydroxyl group at the C3 position of the C ring always considerably diminished the substrate affinity to LPO (see for example quercetin), this effect was stronger for planar flavonoids as compared to the non-planar equivalents. In summary, while the 3,4-dihydroxyphenyl partial structure turned out to be essential for an

efficient regeneration of native LPO, the hydrophobicity of the electron donor (strongly influenced by the residue at the C1 position of the phenyl ring (Fig. 3) and the molecular architecture considerably influence the efficiency to enhance hypothiocyanite production.

In fact, the good binding of phenylethanoids and flavonoids observed in our study can be easily explained by the hydrophobic nature of the LPO substrate channel [3] and is in line with crystallographic docking studies on the binding of aromatic compounds to the enzyme [3,35,36]. Yet it has to be stated that these studies only evaluate the binding of the substrates to native LPO and are not directly transferable to our data where the substrates interact with oxoiron(IV) states (e.g. Compound I* or Compound II) of the enzyme. The results obtained from kinetic studies with LPO and phenolic compounds are also not always comparable to our data as they often use non-physiological conditions (e.g. 500 μM H_2O_2) [37,38]. Still the general structural properties of efficient LPO activity regenerators evaluated in this work are reflected in the literature. Especially phenolic compounds with easily oxidizable hydroxyl groups at the C3 and C4 position were reported to be efficient substrates for activated LPO [37–39].

Moreover, several known LPO inhibitors (e.g. resorcinol) strongly resemble compounds which showed low LPO reactivating properties in our study (e.g. 2,6-dihydroxybenzoic acid). Although not included in Table 1 we also tested 2,4,6-trihydroxybenzoic acid, which turned out as an inhibitor for the $^-$OSCN production by LPO (IC_{50}: 36.7 ± 9.6 μM) under our experimental conditions. The same holds for non-hydroxylated aromatic compounds. For example the flavonoid chrysin (no hydroxylation at the B ring) exhibits an IC_{50} value of 0.23 ± 0.15 μM. Thus it has excellent binding properties but cannot be oxidized by the catalytically active redox intermediates of LPO.

4.4. Reactivity with LPO Compound I and II

The apparent bimolecular rate constants of the reaction between the selected electron donors and Compounds I and II obtained by the stopped-flow measurements are fully in line with the steady-state measurements (compare Tables 1 and 2). From the three investigated substance classes (i.e. benzoic acid, phenylethanoid and cinnamic acid derivatives) the highest rates for reaction with both Compound I and Compound II were obtained for phenylethanoids. Calculated rate constants for Compound II reduction by the corresponding cinnamic acid and benzoic acid derivatives were significantly smaller (factors ∼12–30 and ∼100–600, respectively). Beyond the substance classes the 3,4-dihydroxylated compounds were the best electron donors for Compound II [40,41], which was also reflected by high V_{max} values in the TNB assays.

4.5. Physiological importance

While the chosen concentrations of SCN^- and H_2O_2 meet (patho-)physiological relevant conditions the used amount of enzyme was significantly lower in our in vitro-test system as compared to the conditions in the oral cavity. This deviation from the physiological situation was necessary to be able to perform enzyme-kinetic measurements at a sec to min time scale (see Section 4.1.). A further significant difference to the physiological conditions comes from the fact that we did not include further saliva components, which are known to interact with LPO and to influence its enzymatic activity. One important example for such substances is urate. This compound can be found in concentrations of about 100–200 μM in saliva and is a well-known LPO substrate [42,43]. It was shown that urate efficiently reacts with Compound I of the enzyme (1.1×10^7 M^{-1} s^{-1} at pH 7.0 and 25 °C) while its reactivity

with Compound II is considerably lower (8.5×10^3 M^{-1} s^{-1} at pH 7.0 and 25 °C) [42]. Thus, some Compound II accumulation can be induced by urate, contributing to the disturbance of the (pseudo-)halogenating activity of LPO in the oral cavity. Still as the substrates tested in this study promote the $^-$OSCN-producing activity of LPO by bringing the enzyme from Compound II back to its ferric form it is likely that the results are transferable to the physiological conditions where urate is present. Most interestingly there are reports that under inflammatory conditions the amount of urate in saliva is even reduced as compared to the healthy situation [44].

While this work was performed on the bovine enzyme the high similarities of this enzyme between species make the results well transferable to human LPO [3]. Moreover the presented results may be comparable to other chordata peroxidases, including MPO. In fact, the flavonoid (–)-epicatechin, which emerged as a good LPO activity regenerator, was shown to be an excellent MPO substrate due to its high reactivity with Compound II of this enzyme [15,16]. However, the mechanisms for the H_2O_2-mediated inhibition of the (pseudo-)halogenating activity of LPO and MPO are slightly different [12]. In any case, the present comprehensive study provides an excellent basis for rational intervention in diseases that are known to be accompanied by impaired oxidation of thiocyanate, including dental pathologies and cystic fibrosis [3,11]. The best here identified promotors of hypothiocyanite production could provide the basis as lead compounds for the development of new medications for the stimulation of the humoral defense of the innate immune system under pathological conditions.

5. Conclusion

In body secretions like saliva, tears, milk or airway secretions the heme-containing enzyme lactoperoxidase significantly contributes to the destruction of pathogens by producing hypothiocyanite from thiocyanate. Yet this (pseudo-)halogenating enzyme activity is likely to be impaired under inflammatory conditions. As revealed in this study aromatic compounds with a 3,4-dihydroxyphenyl partial structure are suitable substrates to re-generate the $^-$OSCN production by direct interaction with and reduction of redox intermediates like Compound II. Due to the nature of the substrate binding pocket at the heme cavity, hydrophobic compounds (e.g. phenylethanoids, flavonoids) emerged as better activity promotors of thiocyanate oxidation by LPO. The enzyme-kinetic measurements were performed under simulated conditions of the oral cavity, making the results well transferable to the in vivo situation. Selected stopped-flow kinetic measurements confirmed the obtained data. The presented results provide a basis for the development of new medications for the reactivation of lactoperoxidase activity, which is known to be impaired at different pathological conditions including cystic fibrosis.

Conflict of interest

The authors have no conflict of interest to disclose.

Submission declaration

The data presented here have not been published previously and are currently not under consideration for publication elsewhere.

Acknowledgment

Appendix A. Supplementary material

Supplementary data associated with this article can be found in the online version at http://dx.doi.org/10.1016/j.bbrep.2015.10.001.

References

[1] M. Zámocký, C. Obinger, Molecular phylogeny of heme peroxidases, in: E. Torres, M. Ayala (Eds.), Biocatalysis based on Heme Peroxidases, 1st ed., Springer, Berlin, 2010.

[2] P.G. Furtmuller, M. Zederbauer, W. Jantschko, et al., Active site structure and catalytic mechanisms of human peroxidases, Arch. Biochem. Biophys. 445 (2006) 199–213.

[3] S. Sharma, A.K. Singh, S. Kaushik, et al., Lactoperoxidase: structural insights into the function,ligand binding and inhibition, Int. J. Biochem. Mol. Biol. 4 (2013) 108–128.

[4] N.B. Loughran, B. O'Connor, C. O'Fagain, M.J. O'Connell, The phylogeny of the mammalian heme peroxidases and the evolution of their diverse functions, BMC Evol. Biol. 8 (2008) 101–115.

[5] J. Arnhold, J. Flemmig, Human myeloperoxidase in innate and acquired immunity, Arch. Biochem. Biophys. 500 (2010) 92–106.

[6] J. Wang, A. Slungaard, Role of eosinophil peroxidase in host defense and disease pathology, Arch. Biochem. Biophys. 445 (2006) 256–260.

[7] P.G. Furtmuller, U. Burner, C. Obinger, Reaction of myeloperoxidase compound I with chloride, bromide, iodide, and thiocyanate, Biochemistry 37 (1998) 17923–17930.

[8] P.G. Furtmuller, U. Burner, G. Regelsberger, C. Obinger, Spectral and kinetic studies on the formation of eosinophil peroxidase compound I and its reaction with halides and thiocyanate, Biochemistry 39 (2000) 15578–15584.

[9] P.G. Furtmuller, W. Jantschko, G. Regelsberger, C. Jakopitsch, J. Arnhold, C. Obinger, Reaction of lactoperoxidase compound I with halides and thiocyanate, Biochemistry 41 (2002) 11895–11900.

[10] F. Bafort, O. Parisi, J.P. Perraudin, M.H. Jijakli, Mode of action of lactoperoxidase as related to its antimicrobial activity: a review, Enzyme Res. 2014 (2014) 1–13 (article ID 517164).

[11] Y. Xu, S. Szep, Z. Lu, The antioxidant role of thiocyanate in the pathogenesis of cystic fibrosis and other inflammation-related diseases, Proc. Natl. Acad. Sci. USA 106 (2009) 20515–20519.

[12] J. Flemmig, D. Rusch, M.E. Czerwinska, H.W. Rauwald, J. Arnhold, Components of a standardised olive leaf dry extract (Ph. Eur.) promote hypothiocyanite production by lactoperoxidase, Arch Biochem Biophys 549 (2014) 17–25.

[13] P.G. Furtmuller, J. Arnhold, W. Jantschko, H. Pichler, C. Obinger, Redox properties of the couples compound I/compound II and compound II/native enzyme of human myeloperoxidase, Biochem. Biophys. Res. Commun. 301 (2003) 551–557.

[14] L. Minarowski, D. Sands, A. Minarowska, et al., Thiocyanate concentration in saliva of cystic fibrosis patients, Folia Histochem. Cytobiol. 46 (2008) 245–246.

[15] J. Flemmig, J. Remmler, F. Rohring, J. Arnhold, (−)-Epicatechin regenerates the chlorinating activity of myeloperoxidase in vitro and in neutrophil granulocytes, J. Inorg. Biochem. 130 (2014) 84–91.

[16] H. Spalteholz, P.G. Furtmuller, C. Jakopitsch, et al., Kinetic evidence for rapid oxidation of (−)-epicatechin by human myeloperoxidase, Biochem. Biophys. Res. Commun. 371 (2008) 810–813.

[17] J. Flemmig, I. Noetzel, J. Arnhold, H.W. Rauwald, *Leonurus cardiaca* L. herb extracts and their constituents promote lactoperoxidase activity, J. Funct. Foods 17 (2015) 328–339.

[18] K. Wojtyniak, M. Szymanski, I. Matlawska, Leonurus cardiaca L. (motherwort): a review of its phytochemistry and pharmacology, Phytother. Res. 27 (2013) 1115–1120.

[19] E. Tripoli, M. Giammanco, G. Tabacchi, M.D. Di, S. Giammanco, G.M. La, The phenolic compounds of olive oil: structure, biological activity and beneficial effects on human health, Nutr. Res. Rev. 18 (2005) 98–112.

[20] R.F. Beers Jr., I.W. Sizer, A spectrophotometric method for measuring the breakdown of hydrogen peroxide by catalase, J. Biol. Chem. 195 (1952) 133–140.

[21] C.J. van Dalen, M.W. Whitehouse, C.C. Winterbourn, A.J. Kettle, Thiocyanate and chloride as competing substrates for myeloperoxidase, Biochem. J. 327 (1997) 487–492.

[22] P.G. Furtmuller, J. Arnhold, W. Jantschko, M. Zederbauer, C. Jakopitsch, C. Obinger, Standard reduction potentials of all couples of the peroxidase cycle of lactoperoxidase, J. Inorg. Biochem. 99 (2005) 1220–1229.

[23] K.M. Pruitt, J. Tenovuo, B. Mansson-Rahemtulla, P. Harrington, D.C. Baldone, Is thiocyanate peroxidation at equilibrium in vivo? Biochim. Biophys. Acta 870 (1986) 385–391.

[24] P. Nagy, G.N. Jameson, C.C. Winterbourn, Kinetics and mechanisms of the reaction of hypothiocyanous acid with 5-thio-2-nitrobenzoic acid and reduced glutathione, Chem. Res. Toxicol. 22 (2009) 1833–1840.

[25] W. Jantschko, P.G. Furtmuller, M. Allegra, et al., Redox intermediates of plant and mammalian peroxidases: a comparative transient-kinetic study of their reactivity toward indole derivatives, Arch. Biochem. Biophys. 398 (2002) 12–22.

[26] M. Sisecioglu, M. Cankaya, I. Gulcin, H. Ozdemir, The inhibitory effect of propofol on bovine lactoperoxidase, Protein Pept. Lett. 16 (2009) 46–49.

[27] M.R. Clausen, L.H. Skibsted, J. Stagsted, Inhibition of lactoperoxidase-catalyzed 2,2′-azino-bis(3-ethylbenzthiazoline-6-sulfonic acid) (ABTS) and tyrosine oxidation by tyrosine-containing random amino acid copolymers, J. Agric. Food Chem. 56 (2008) 8692–8698.

[28] M. Sisecioglu, M. Cankaya, H. Ozdemir, Effects of some vitamins on lactoperoxidase enzyme activity, Int. J. Vitam. Nutr. Res. 79 (2009) 188–194.

[29] J.D. Chandler, B.J. Day, Thiocyanate: a potentially useful therapeutic agent with host defense and antioxidant properties, Biochem. Pharmacol. 84 (2012) 1381–1387.

[30] G.E. Conner, C. Wijkstrom-Frei, S.H. Randell, V.E. Fernandez, M. Salathe, The lactoperoxidase system links anion transport to host defense in cystic fibrosis, FEBS Lett. 581 (2007) 271–278.

[31] W. Jantschko, P.G. Furtmuller, M. Zederbauer, K. Neugschwandtner, C. Jakopitsch, C. Obinger, Reaction of ferrous lactoperoxidase with hydrogen peroxide and dioxygen: an anaerobic stopped-flow study, Arch. Biochem. Biophys. 434 (2005) 51–59.

[32] J. Vlasits, C. Jakopitsch, M. Bernroitner, M. Zamocky, P.G. Furtmuller, C. Obinger, Mechanisms of catalase activity of heme peroxidases, Arch. Biochem. Biophys. 500 (2010) 74–81.

[33] H. Jenzer, H. Kohler, C. Broger, The role of hydroxyl radicals in irreversible inactivation of lactoperoxidase by excess H$_2$O$_2$. A spin-trapping/ESR and absorption spectroscopy study, Arch. Biochem. Biophys. 258 (1987) 381–390.

[34] H. Kohler, H. Jenzer, Interaction of lactoperoxidase with hydrogen peroxide. Formation of enzyme intermediates and generation of free radicals, Free Radic. Biol. Med. 6 (1989) 323–339.

[35] A.K. Singh, N. Singh, A. Tiwari, et al., First structural evidence for the mode of diffusion of aromatic ligands and ligand-induced closure of the hydrophobic channel in heme peroxidases, J. Biol. Inorg. Chem. 15 (2010) 1099–1107.

[36] A.K. Singh, N. Singh, M. Sinha, et al., Binding modes of aromatic ligands to mammalian heme peroxidases with associated functional implications: crystal structures of lactoperoxidase complexes with acetylsalicylic acid, salicylhydroxamic acid, and benzylhydroxamic acid, J. Biol. Chem. 284 (2009) 20311–20318.

[37] E. Monzani, A.L. Gatti, A. Profumo, L. Casella, M. Gullotti, Oxidation of phenolic compounds by lactoperoxidase. Evidence for the presence of a low-potential compound II during catalytic turnover, Biochemistry 36 (1997) 1918–1926.

[38] G.G. Oakley, U. Devanaboyina, L.W. Robertson, R.C. Gupta, Oxidative DNA damage induced by activation of polychlorinated biphenyls (PCBs): implications for PCB-induced oxidative stress in breast cancer, Chem. Res. Toxicol. 9 (1996) 1285–1292.

[39] R.P. Ferrari, E. Laurenti, Oxidation of catechols and catecholamines by horseradish peroxidase and lactoperoxidase: ESR spin stabilization approach combined with optical methods, Spectrochim. Acta: A 49 (1993) 1261–1267.

[40] P.G. Furtmuller, U. Burner, W. Jantschko, G. Regelsberger, C. Obinger, Twoelectron reduction and one-electron oxidation of organic hydroperoxides by human myeloperoxidase, FEBS Lett. 484 (2000) 139–143.

[41] K.W. Zuurbier, A.R. Bakkenist, R. Wever, A.O. Muijsers, The chlorinating activity of human myeloperoxidase: high initial activity at neutral pH value and activation by electron donors, Biochim. Biophys. Acta 1037 (1990) 140–146.

[42] A. Seidel, H. Parker, R. Turner, et al., Uric acid and thiocyanate as competing substrates of lactoperoxidase, J. Biol. Chem. 289 (2014) 21937–21949.

[43] S. Moore, K.A. Calder, N.J. Miller, C.A. Rice-Evans, Antioxidant activity of saliva and periodontal disease, Free Radic. Res. 21 (1994) 417–425.

[44] S. Liskmann, T. Vihalemm, O. Salum, K. Zilmer, K. Fischer, M. Zilmer, Characterization of the antioxidant profile of human saliva in peri-implant health and disease, Clin. Oral Implants Res. 18 (2007) 27–33.